Numerical Simulation and Experiment on Thin-Shell Object Separation from Aircraft

Liang Shibo(梁世波)*, *Wang Yang*(王阳), *Xia Jian*(夏健)

UAV Research Institute, Nanjing University of Aeronautics and Astronautics, Nanjing 210016, P. R. China

(Received 11 November 2014; revised 3 January 2015; accepted 12 January 2015)

Abstract: The unsteady aerodynamic loads generated by the thin-shell object separating from aircraft affects flying safety. To investigate the loads, a method combining numerical simulation and experiment is proposed. Firstly, the motional tendency of the thin-shell object separating from aircraft is calculated, and then the high-speed air blowing test on ground is designed. Thereafter, the external store is employed to avoid colliding with the thin-shell object in air. Finally, the hanging and flight test is conducted by a high-speed unmanned aerial vehicle (UAV), and the feasibility of the thin-shell object separating from aircraft at high speed is proved. Consequently, the separating problem of a thin-shell object with an unconventional aerodynamic configuration is solved, and the collisions with aircraft is prevented.

Key words: external stores; thin-shell object; external stores separation; unstructured overset grid

CLC number: V211.71 **Document code**: A **Article ID**: 1005-1120(2015)01-0089-08

0 Introduction

The external store is an essential supplement to extend the function of aircrafts, and the whole or partial separation is an effective way to realize the function. At the beginning of separation, due to the flow field around, the nacelle is influenced by the force or moment, then the results of separation are greatly affected, which may sometimes threaten aircraft flying safety. Thus, analysis of the interference effects of separating part is important. The aerodynamic problems, especially those on the external pod with complex or unconventional aerodynamic shape, are particularly prominent, and the calculation analysis and test research on the separation process are practical and effective.

The computational fluid dynamics (CFD) method is mostly adopted in aerodynamic analysis for the separation of aircraft external hanging nacelle[1-2]. By the use of overset grid and Euler equations, good results are obtained when analyzed the objects with excellent aerodynamic shapes[3-5], such as auxiliary fuel tanks and missiles. The research of external stores separation with conventional shape is usually based on structured grids, whose topological relation is simple, and easy to generate body-fitted grid. The nodes between the overset grids are corresponding to each grid after the formation of the grid, which ensures the data exchange between overset grids. However, it is difficult for the structured grid to be blocked. Especially for the objects with complex shapes, it is difficult to generate and apply the structured grid. As for unstructured grid it has unique advantages of flexibility in managing the objects with complex shapes. Therefore, the flow around a complex shape object can be analyzed by solving the Euler and Navier-Stokes (N-S) equations on the unstructured grid, thus reducing the computational complexity[6]. Generally, unstructured grid is suitable for calculating and analyzing external stores with unconventional

* **Corresponding author**: Liang Shibo, Associate Researcher, E-mail: liangsb@nuaa.edu.cn.

How to cite this article: Liang Shibo, Wang Yang, Xia Jian. Numerical simulation and experiment on thin-shell object separation from aircraft[J]. Trans. Nanjing U. Aero. Astro., 2015,32(1):89-96.
http://dx.doi.org/10.16356/j.1005-1120.2015.01.089

aerodynamic configuration.

Considering few documented researches on the separation of a thin-shell object preciously, this paper focuses on exploring this issue practically.

Here, the separation of thin shell object with unconventional aerodynamic configuration from aircraft is studied, during which unsteady aerodynamic interactions are particularly outstanding. Due to the poor reliability of sole theoretical calculation, a method combing numerical calculation and experimental research is developed to improve the low accuracy, and to avoid the interaction between the aircraft and a separated thin-shell object. Unstructured overset grids[7-10] and dual-time step[11-12] are adopted in the numerical calculation, which absorb both advantages of the unstructured grid in dealing with complex shape and of the overset grid in solving separation between aircraft and external store in air. Then the process of separation between aircraft and a thin-shell object with unconventional aerodynamic configuration is calculated. In order to improve the calculation accuracy and to reduce the flight tests at risk, a high-speed air blowing test on ground is firstly conducted. After the test, the calculation results are modified. Finally, the hanging and flight test is carried out by a high speed UAV. It is shown that the developed method is highly effective for the study on the separation of thin-shell object in air.

1 Numerical Method

To investigate the separation process of a thin-shell object from aircraft, the N-S equations based on unstructured overset grid method are selected as the governing equations. By calculating unsteady Euler/N-S and 6-DOF motion equations of rigid body, a numerical method based on unstructured overset grid and simulation of the flow around body is developed to study the characteristics of the flowfield around the objects with relative motion.

1.1 Governing equations

The three-dimensional compressible N-S[13] equations in integral form in moving meshes can be written as

$$\frac{\partial}{\partial t}\int_{\Omega}\boldsymbol{W}\mathrm{d}\Omega+\oint_{\partial\Omega}(\boldsymbol{F}_c-\boldsymbol{F}_v)\mathrm{d}s=0 \tag{1}$$

where

$$\boldsymbol{W}=\begin{bmatrix}\rho\\ \rho u\\ \rho v\\ \rho w\\ \rho E\end{bmatrix},\quad \boldsymbol{F}_c=\begin{bmatrix}\rho V_r\\ \rho u V_r+pn_x\\ \rho v V_r+pn_y\\ \rho w V_r+pn_z\\ \rho H V_r+pV_b\end{bmatrix}$$

$$\boldsymbol{F}_v=\begin{bmatrix}0\\ \tau_{xx}n_x+\tau_{xy}n_y+\tau_{xz}n_z\\ \tau_{yx}n_x+\tau_{yy}n_y+\tau_{yz}n_z\\ \tau_{zx}n_x+\tau_{zy}n_y+\tau_{zz}n_z\\ \Theta_x n_x+\Theta_y n_y+\Theta_z n_z\end{bmatrix}$$

where ρ, p, E and H stand for the density, pressure, unit mass energy and unit mass enthalpy of fluid respectively, and u, v, w are the velocity components along the x, y, z direction, respectively. V_r is the normal velocity of fluid and grids, τ_{ij} the viscous stress tensor, and Θ_i the combination of viscous stress power and heat conduction.

1.2 Time marching method

A dual-time stepping method is applied to simulate the unsteady flow phenomenon. In this method, the LU-SGS scheme[14] based on grid rearrangement technique is employed at every pseudo-time step, which can be written as

Forward sweeping of LU-SGS

$$\Delta W^*=D^{-1}\left[\mathrm{RHS}^m-\frac{1}{2}\sum_{j(i)}\Delta S(\Delta F^*-\rho_A\Delta W^*)\right] \tag{2}$$

Backwards sweeping of LU-SGS

$$\Delta W^m=\Delta W^*-\frac{1}{2}D^{-1}\sum_{j(i)}\Delta S(\Delta F^*-\rho_A\Delta W^m) \tag{3}$$

where

$$D=\left(\frac{\Omega}{\Delta\tau}+\frac{3\Omega}{2\Delta t}+\frac{1}{2}\sum_{j(i)}\Delta S\rho_A\right)I$$

$$\mathrm{RHS}^m=-\sum_{j(i)}\Delta S(F^m(W)-G^m(W))-\frac{3W^{n,m}\Omega^n-4W^n\Omega^n+W^{n-1}\Omega^{n-1}}{2\Delta t}$$

where n indicates the real-time step, and m the pseudo-time step. The specific expressions of Eqs. (2,3) can be referred to Ref. [14].

1.3 Surface function

The White-Christoph[15] compressible surface function used in this paper can be written as

$$u^+=\frac{1}{2\gamma}\left\{\beta+Q\sin\left(\phi+\frac{\sqrt{\gamma}}{\kappa}\left[2(S-S_0)+\ln\left(\frac{S-1}{S+1}\cdot\frac{S_0+1}{S_0-1}\right)\right]\right)\right\} \tag{4}$$

where

$$\phi=\arcsin^{-1}\frac{-\beta}{Q},\ Q=\sqrt{\beta^2+4\gamma},\ S=\sqrt{1+ay^+},$$

$$a=\frac{v_1(\mathrm{d}p/\mathrm{d}s)_{\mathrm{wall}}}{\tau_1 u_\tau},\ \beta=\frac{q_{\mathrm{wall}}v_1}{T_1 k_1 u_\tau},\ \gamma=\frac{(Pr)^{1/3}u_\tau^2}{2C_pT_1}$$

Here, α, β, γ, ϕ, Q, S indicate the constants of the model boundary conditions. The specific expressions of Eqs. (2, 3) can be found in Ref. [15].

1.4 Grid system

The isolated points are simply cleared in structured overset grids, which may lead to the poor quality of grid boundary. Therefore, an optimized method is applied to classify grid nodes and define grid boundary[16]. The definition of grid boundary is divided into two steps, in which different classification parameters are used. Consequently, an optimized grid boundary can be obtained. The overall carrier grid generated in this paper is shown in Fig. 1.

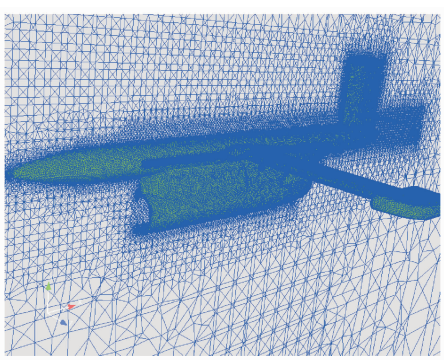

Fig. 1 Overall grid of a carrier

The model of hatch cover of nacelle external store is shown in Fig. 2, which will separate from aircraft in a certain speed.

1.5 Calculation steps

Fig. 3 illustrates the flow chart of unsteady flowfield calculation based on the unstructured grid, mainly consisting of four modules: information reading module, grid processing module, flowfield calculating module, and data output module.

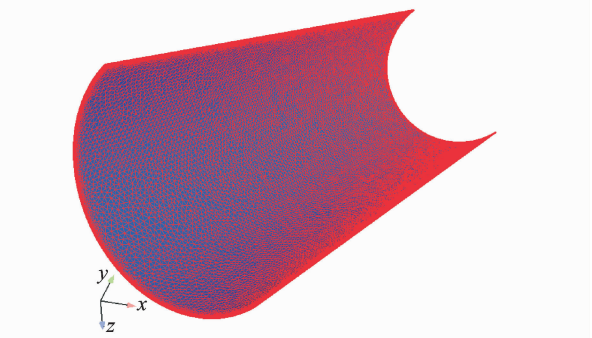

Fig. 2 Grid of hatch cover of nacelle external store

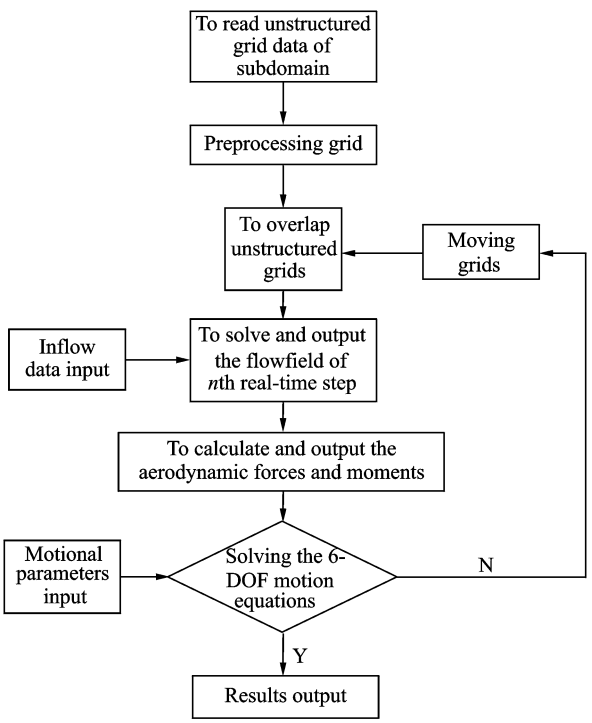

Fig. 3 Flow chart of unsteady flowfield calculation based on unstructured grid

Dynamic calculation steps of unsteady flowfield based on the unstructured grid are as follows:

Step 1 To read unstructured grid data of subdomain;

Step 2 To obtain relevant data of unstructured overset grid and flowfield calculation by preprocessing grid of subdomain;

Step 3 To overlap unstructured grids, in-

cluding donor cell searching, interpolation boundary confirming and nodes classifying;

Step 4 To solve and output the flowfield of nth real-time step;

Step 5 To calculate and output the aerodynamic forces and moments under the current condition;

Step 6 To obtain the motion parameters on $(n+1)$ th real-time step by solving the 6-DOF motion equations.

Step 7 To modify grid and motion information according to the data received in step 6);

Step 8 To repeat Steps 3—7 until the convergence occures.

2 Numerical Examples

For requirements of the flight environment and the use of UAV, the flight conditions are set to be the same in the two numerical examples. Then the comparison of different separation speeds of the hatch cover from UAV is analyzed so as to study the optimum speed of the separation under the given conditions.

The parameters of the hatch cover are as follows: weight 11.4 kg; center of gravity (0.949, 0.16, 0.09), with the origin located at the center of disk; inertias $I_{xx}=0.465$ kg·m^2, $I_{yy}=4.028$ kg·m^2, $I_{zz}=3.713$ kg·m^2.

Computational cases under a variety of conditions are conducted, and two representative examples are presented here.

2.1 Case 1 with initial separation speed of 3.5 m/s

Calculation conditions are listed as follows: the initial separation speed 3.5 m/s, the angle of side slip 0°, the flight altitude 500 m, the flight velocity 780 km/h, the initial attack angle 0°, and the real-time step 0.002 5 s.

Fig. 4 shows the time history of aerodynamic moments and mass center velocities during the separation. Fig. 5 shows the evolution of the hatch cover during separation process.

When the hatch cover is moving down at an initial release speed of 3.5 m/s, the pitch aerodynamic moment is negative, then the head raising motion of the hatch cover appeares. The angle of

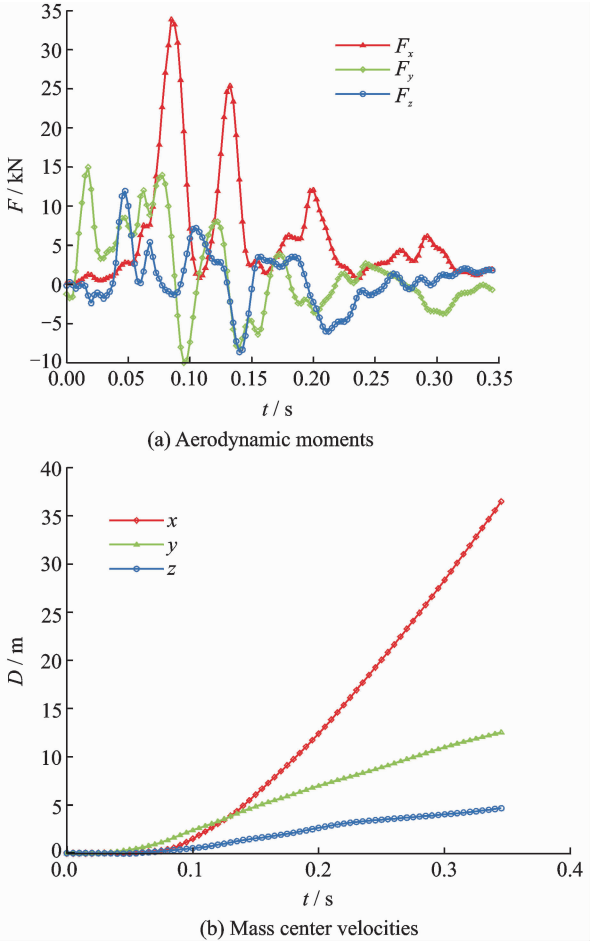

Fig. 4 Time history of aerodynamic moments and mass center velocities during separation with initial separation speed of 3.5 m/s

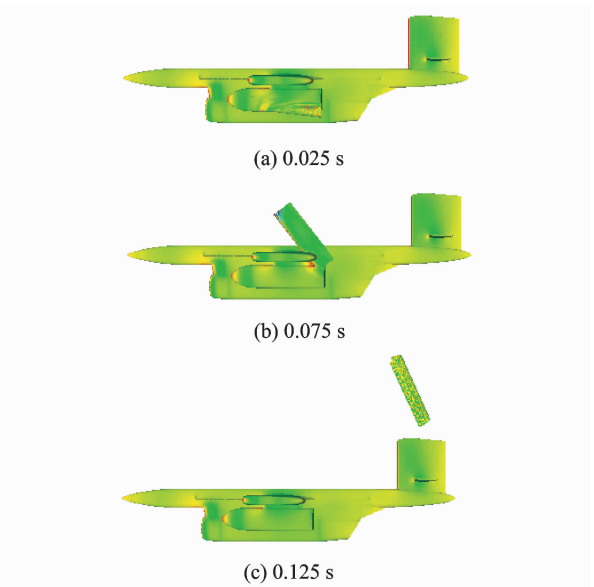

Fig. 5 Evolution process of hatch cover during separation with initial separation speed of 3.5 m/s

head raising amplifies quickly because the moment of inertia of the hatch cover is small, and then the hatch cover collides with the external store, which is dangerous for flight safety.

2.2 Case 2 with initial separation speed of 5 m/s

The initial separation speed is 5 m/s, the angle of side slip 0°, the flight altitude 500 m, the flight velocity 780 km/h, the initial attack angle 0°, and the real time step 0.002 5 s.

Fig. 6 shows the time history of aerodynamic moments and mass center velocities during the separation. Fig. 7 shows the evolution process of the hatch cover during separation.

Numerical results show that the hatch cover can be separated smoothly if the initial separation speed is set as 5 m/s. It indicates that the initial separation speed of hatch cover has a significant effect on separation safety.

At the initial separation speed of 5 m/s with the angle of side slip of 0°, setting the pitch angular velocity as 1°/s (nose-down), Fig. 8 shows the motion of the hatch cover during the process. Results show that setting a pitch angular velocity (nose-down) is beneficial for the separation of the

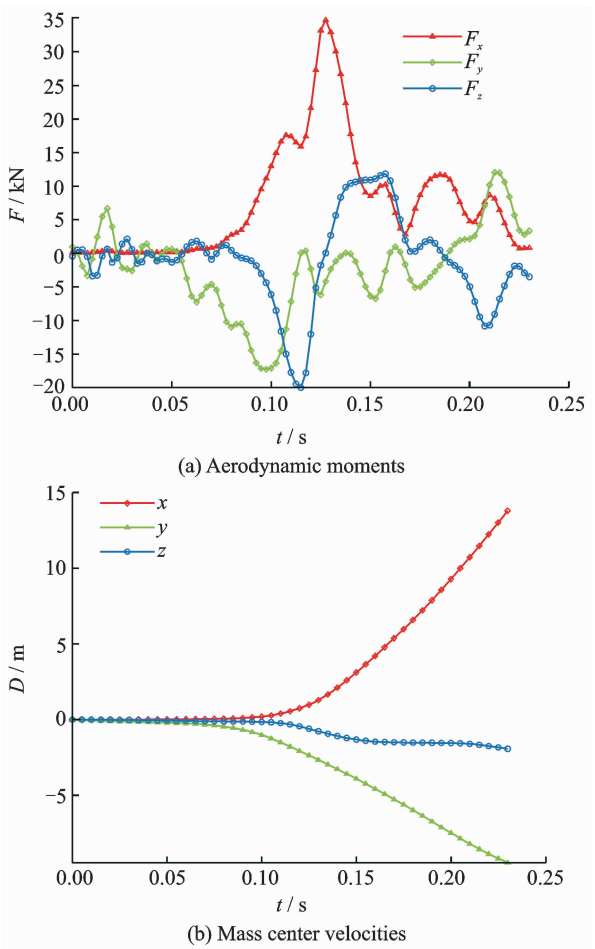

Fig. 6 Time history of aerodynamic moments and mass center velocities during the the separation with initial separation speed of 5 m/s

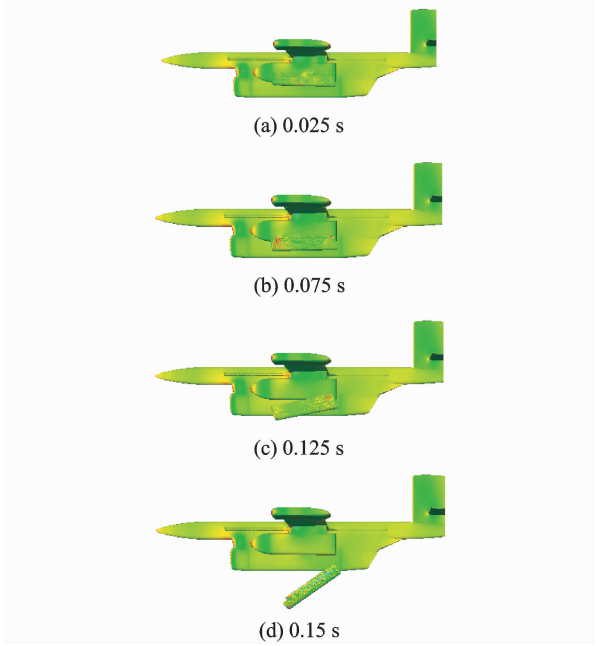

Fig. 7 Evolution process of hatch cover during separation with initial separation speed of 5 m/s

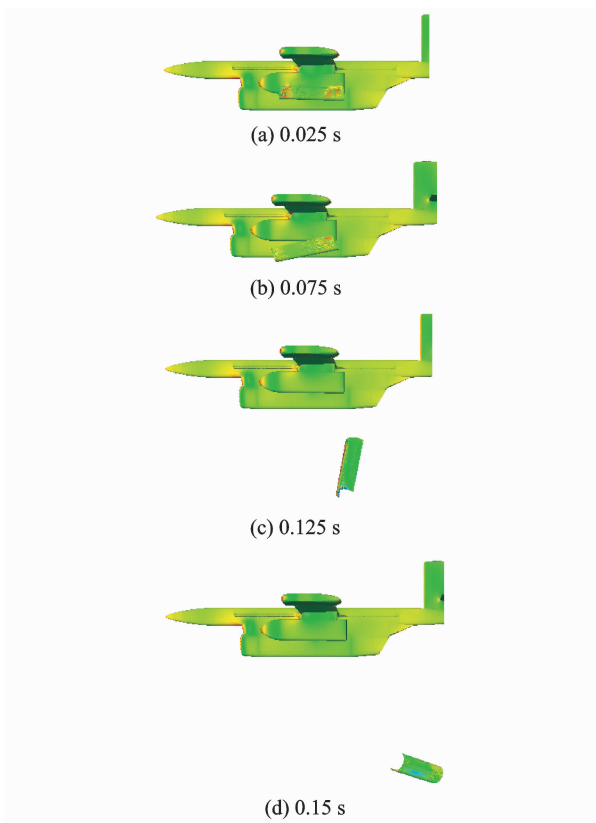

Fig. 8 Motion of hatch cover during separation process with initial separation speed of 5 m/s and 1 °/s pitch angular velocity of nose-down

hatch cover and body, and can result in a gain in flight safety.

3 Tests

According to the results of numerical calculation, an experiment is designed to reveal the separation mechanism of a hatch cover, and tests on ground and in flight are separately conducted.

3.1 High-speed air blowing test on ground

For reducing the risk in flight tests, a high-speed air blowing experiment is conducted on ground to amend the numerical results and to improve the success rate of hatch cover separation from external store.

Fig. 9 shows the process of high-speed air blowing test on ground recorded by a camera. Thus the separation velocity can be adjusted according to the actual condition.

In the air blowing test on ground, the numerical value of the velocity at which the hatch cover starts to separate is larger than the one obtained from the test, indicating that the secure separation velocity of the hatch cover can be revised to 6 m/s.

3.2 Hanging and flight test

The external store is hanged on the high speed UAV at a flying speed of 780 km/h with the angle of side slip of 0°. The hatch cover is thrown at the speed of 5 m/s. Fig. 10 shows the process of separation, where the hatch cover separates from the store rapidly without any collision with them.

Fig. 11 shows the comparison between the numerical and flight test results. It demonstrates that there is a slight difference between the results of numerical simulation and flight test. In the flight test, the motion trajectory of hatch cover is straighter. It means that the results of numerical calculation are larger than that of the real situation.

The theoretical value should be modified because the unsteady aerodynamic loads cannot be accurately simulated. Therefore, the turbulence model should be further studied. And it is necessary for the tests on ground and in flight with respect to the thin-shell object separation from external store.

(a) Blowing

(b) Separating process

(c) Separated state

Fig. 9 Process of high-speed air blowing test on ground

4 Conclusions

Numerical simulation and experimental method are proposed to investigate the separation of a thin-shell object from aircraft. Analyzing the previous data of flight tests and results of calculation, the following conclusions can be drawn:

(1) The movement of hatch cover during the separation in air is greatly affected by the initial separation speed and pitch angular velocity. The faster the initial separation speed and pitch angular velocity, the safer the separation.

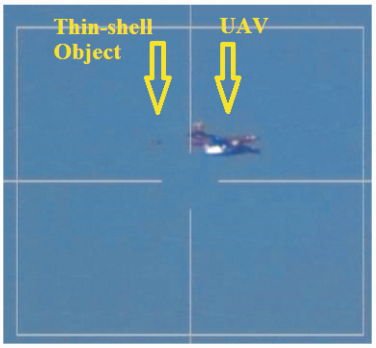

(a)

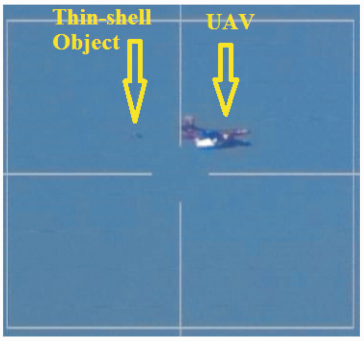

(b)

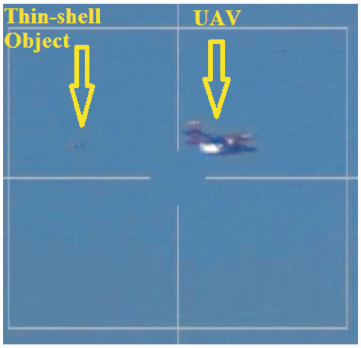

(c)

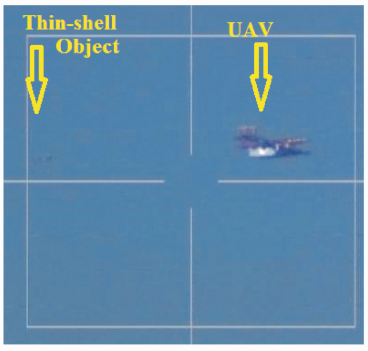

(d)

Fig. 10 Separation process of hatch cover at bottom of store

(2) By the combination of calculation and measurement both on ground and in flight, the separation of thin-shell object with unconventional aerodynamic configuration in air can be solved effectively.

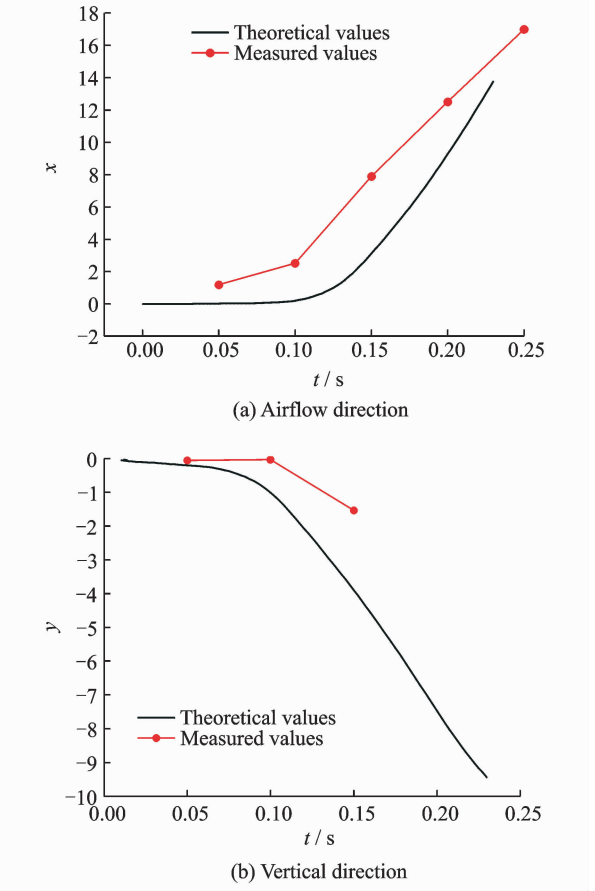

Fig. 11 Comparison between numerical calculation and flight test

(3) Based on the unstructured overset grid, the separation of thin-shell object from unconventional aerodynamic configuration can be numerically simulated, thus presenting an initial design benchmark of separation mechanism.

Acknowledgement

This work was supported by the Fundamental Research Funds for the Central Universities (No. XZA14027).

References:

[1] Glowinski R, Pan Tsorng-Whay, Periaux J. Numerical simulation of a multi-store separation phenomenon: A fictitious domain approach[J]. Computer Methods in Applied Mechanics and Engineering, 2006,195(41/42/43):5566-5581.

[2] Gao Shuyi, Wang Haitao, Cheng Wenke, et al. Ejection separation characteristic analysis of parachute container cover from return capsule for lunar

exploration [J]. Transactions of Nanjing University of Aeronautics and Astronautics, 2014,31(5):552-558.

[3] Lee C J, Getson E. IHAAA applications to reducing store separation flight testing[R]. AIAA-2007-l653, 2007.

[4] Harish G, Pavanakumar M. Store separation dynamics using grid-free Euler solver[R]. AIAA-2006-3650, 2006.

[5] Shi Yongjie, Xu Guohua, Wang Fei. Propagation characteristics of helicopter rotor blade—vortex interaction noise[J]. Journal of Nanjing University of Aeronautics & Astronautics, 2014,46(2):212-217. (in Chinese)

[6] Ye Liang, Zhao Qijun, Xu Guohua. An adaptive unstructured embedded mesh methodology suitable for the calculation on the rotor vortex flowfield[J]. Acta Aerodynamica Sinica, 2008,26(3):214-218. (in Chinese)

[7] Nakahashi K, Fumiya T. An intergrid boundary definition method for overset unstructured grid approach [R]. AIAA-L09-3304, 1999.

[8] Togashi F, Nakahashi K, Ito Y. Flow simulation of NAL experimental supersonic airplane/booster separation using overset unstructured 96ds[R]. AIAA-2000-1007, 2000.

[9] Frink N T. Recent progress towards a three-dimensional unstructured Navier-Stokes flow solver, AIAA-94-0061, 1994.

[10] Hilgenstock A. A fast method for the elliptic generation of three-dimensional grids with full boundary control[C]// Numerical Grid Generation in CFM′88 C, Proceedings of the Second International Conference. Miami Beach, USA: Pineridge Press, 1988.

[11] Blazek J. Computational fluid dynamics z principle and applications[M]. Oxford: Elsevier, 2001: 142-145.

[12] Luo H. A fast matrix-free implicit method for computing low Mach number flows on unstructured grids [R]. AIAA-99-3315, 1999.

[13] Fan F, Shi Y J, Xu G H. Computational research on aerodynamic and aeroacoustic characteristics of scissors tail-rotor in hover[J]. Acta Aeronautica et Astronautica Ainica, 2013,34(9): 2100-2109. (in Chinese)

[14] Luo H, Baum J D. A fast, matrix-free implicit method for computing low Mach number flows on unstructured grids[R]. AIAA-99-3315, 1999.

[15] Mani M. A compressible wall function for steady and unsteady flow applications [R]. AIAA-99-3216, 1999.

[16] Nakahashi K, Gumiya T. An intergrid boundary definition method for overset unstructured grid approach [R]. AIAA-99-3304, 1999.

(Executive editor: Zhang Tong)